Fusion Engineering and Design 218 (2025) 115184

Contents lists available at ScienceDirect

Fusion Engineering and Design

journal homepage: www.elsevier.com/locate/fusengdes

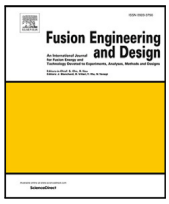

Activity assessment in water coolant loops and rooms using the SAETTA tritium transport code

Federico Hattab [a,*], Vincenzo Narcisi [b], Cristiano Ciurluini [a], Fabio Giannetti [a], Giulia Valeria Centomani [c], Antonio Trotta [c], Alessia Santucci [b]

[a] Nuclear Engineering Research Group, DIAEE - Sapienza University of Rome, Corso Vittorio Emanuele II 244, 00186 Rome, Italy
[b] ENEA, Nuclear Department, Via E. Fermi 45, 00044, Frascati, Italy
[c] Eni S.p.A., MAFE, Venice 30175, Italy

ARTICLE INFO

Keywords:
EU-DEMO
Water-Cooled Lead–Lithium
Tritium permeation
Primary Heat Transfer System
Python

ABSTRACT

The management of hydrogen isotopes within a tokamak fusion reactor presents a significant design challenge, particularly with respect to tritium management. It is essential for the fusion power plant to achieve self-sufficiency in its fuel supply while minimizing component contamination and external releases. This study presents an analysis of tritium migration within the EU DEMO Water-Cooled Lead–Lithium (WCLL) Breeding Blanket (BB) Primary Heat Transfer System (PHTS). The objective is to evaluate tritium inventories and release rates from the primary circuit to the tokamak building. The assessment utilizes SAETTA, a validated system-level tritium transport code, able to describe several physical phenomena in a variety of medium and structural components. A versatile PHTS model has been developed, allowing for relatively rapid yet detailed sensitivity analyses on specific parameters. The tritium inventory in the primary coolant and connected rooms has been estimated, along with loss rates.

Key factors impacting inventories and losses under reference conditions include the size of the Coolant Purification System (CPS) and potential leaks from piping. Additionally, the study discusses the acceptable limits for tritium concentration in the air. The effects of leaks, CPS size, hydrogen concentration in the water, and Permeation Reduction Factors (PRF) at the steam generator walls have also been evaluated. The findings from this analysis will aid in optimizing the PHTS circuit design, defining tritium management and room ventilation strategies, and informing the design of fuel cycle components by providing necessary source terms.

1. Introduction

The European DEMOnstration power plant (EU DEMO) is tasked to prove the viability of magnetic confinement fusion from a technological and industrial point of view. Tritium self-sufficiency must be achieved and net, safe and reliable power must be delivered to the grid [1]. In a typical tokamak device, tritium is generated in the Breeding Blanket (BB) via reactions between lithium and neutrons coming from the plasma chamber. The breeding is enhanced by the presence of a neutron multiplier, usually lead or beryllium. Due to the significant deposition of energy, the BB needs to be actively cooled by the Primary Heat Transfer System (PHTS) [1]. The latter is part of the reactor Balance of Plant (BoP), which encompasses the systems responsible for the removal of plasma power and its conversion into electricity. Tritium can permeate from the BB to the PHTS, contaminating the coolant and structures. A portion of the tritium in the PHTS is removed by the Coolant Purification System (CPS), while another fraction is lost via permeation and leaks. The two main pathways associated with these losses are through the primary piping towards the corresponding rooms of the Tokamak Building and through the tubes of the Steam Generators (SGs) towards the Power Conversion System (PCS). Mitigation strategies such as the use of anti-permeation barriers and welded joints for piping can be used to reduce the amount of tritium lost from the primary coolant [2]. Depending on the tritium concentration in the Tokamak Building rooms, it could be necessary to send the ambient air to an Exhaust Detritiation System (EDS) before releasing it to the stack, while the liquid (tritiated) lost from the PHTS is collected in storage tanks via a sump system. Losses from the PHTS affect loads to detritiation systems, which are typically large and costly components. Knowing the magnitude and cause of these losses can prove useful for the optimization of the plant design, for the definition of appropriate mitigation strategies and to reduce loads to critical components.

Due to the high complexity of DEMO, and leveraging experience from ITER design and construction, the EUROfusion consortium has

* Corresponding author.
E-mail address: federico.hattab@uniroma1.it (F. Hattab).

https://doi.org/10.1016/j.fusengdes.2025.115184
Received 1 December 2024; Received in revised form 9 April 2025; Accepted 9 May 2025
Available online 28 May 2025

identified eight Key Design Integration Issues (KDIIs) [3] which are integration topics that need focused efforts. In this regard, the KDII2 addresses integration issues related to the BB and its ancillary systems. One area of assessment is the safety impact of the BB design and of its auxiliaries, for which tritium analysis works have been carried out. In 2021, tritium inventories and permeation rates in the BB system have been estimated for the Helium-Cooled Pebble Bed (HCPB) and the Water-Cooled Lead–Lithium (WCLL) BB variants. The FUS-TPC code [4] was used, a purpose built MATLAB application employing a 0D approach for rapid assessments. Concerning the WCLL variant, a key takeaway was the need for an in-line CPS for minimizing tritium inventory in the coolant and thus losses from the PHTS. Previous system-level studies on the HCPB variant have been conducted utilizing the EcosimPro software [5], which is a simulation tool for modelling continuous-discrete systems and includes a collection of tritium transport libraries. Other works [6,7] presented dedicated numerical models for the WCLL and for the Helium-Cooled Lithium Lead blanket. More recently, tritium transport analysis of the BB based on the Double-Coolant Lithium-Lead concept have been made using EcosimPro [8]. The lead–lithium loop related to one BB sector was analysed to investigate the effect of ceramic materials on tritium permeation. An highlight from this work was how the increase of H_2 concentration in the water of the heat exchanger reduces permeation from the lead–lithium loop.

The goal of this work is to estimate tritium inventories and loss rates in the most recent WCLL BB PHTS configuration, as well as the activity levels in the associated tokamak building rooms, utilizing the 1D system-level code SAETTA [9]. The code is lightweight, fully developed on top of open-source software, and has undergone a comprehensive verification and validation process. The flexible architecture of SAETTA allows for plant-wide simulations while maintaining all relevant data and without compromising on spatial and temporal resolution. New configurations for the CPS have been evaluated, and the impact of H_2 concentration on the water loop and losses to the surrounding rooms has been analysed.

The results of this type of analysis can provide valuable insights for fuel cycle process simulations, such as those conducted by [10,11] using Aspen Custom Modeler. A crucial aspect of fuel cycle modelling is the knowledge of hydrogen flows coming from outside the tritium plant and the plant-level analysis here presented can provide these estimations.

2. Modelling work

The tritium transport analysis is carried out using the SAETTA tritium transport code [9]. The Python-based application has been developed to perform general-purpose tritium transport analysis and has been verified and validated for fusion applications [9]. Base components can be connected together to model complex systems. The main hydrodynamic components are pipes, a succession of fluid volumes connected together to simulate 1D fluid flow within a closed channel. Pipes can be connected to structures, where hydrogen diffusion-trapping is computed implicitly (see [9] for further details). Depending on the options chosen in the input file, the simulation can be tailored to the specific application. For instance, following a preliminary assessment of the permeation regime in the PHTS, it was chosen to neglect (turn-off in the model) surface effects and tritium mass transfer from the bulk of the water to the internal piping walls.

The BB PHTS nodalization is shown in Fig. 1. The piping is modelled with 1D pipes, which are connected to the inner side of cylindrical structures to simulate permeation and leakage. On the outer side of each structure one of the three rooms under analysis is connected, with the exception of the U-Tube SGs (UTSGs), which are connected to the Power Conversion System (PCS), and the BB, modelled as a pipe with no walls and no losses. The inherent design of SGs, i.e. large and thin surfaces at high temperatures, makes them prone to significant tritium permeation fluxes. To mitigate this phenomena, anti-permeation barriers and/or natural oxide layers are used [2]. The effect of these barrier is usually quantified with a Permeation Reduction Factor (PRF), defined as the ratio between the permeation flux thorough the uncoated material and that through the coated one (Eq. (1)).

$$\mathrm{PRF} = \frac{J_{\mathrm{p,uncoated}}}{J_{\mathrm{p,coated}}} \tag{1}$$

A source term within the BB volume models the permeation of tritium from the lead–lithium to the water loop. For a more detailed description of the system refer to Section 3.1. In the water loop, tritium may undergo decay, be extracted in the CPS, or permeate/leak into the tokamak building rooms and the power conversion system. A schematic of these different pathways is shown in Fig. 2.

Four hydrogen compounds are considered: HT, H_2, HTO and H_2O (T_2 and T_2O are neglected since it is assumed that almost all T is in HT form) and the chemical reaction in Eq. (2) is considered.

$$H_2O + HT \rightarrow HTO + H_2 \tag{2}$$

The conservation equation used for HT inside pipe volumes is shown in Eq. (3). Analogous equations are considered for the other species, with the differences that HTO and H_2O do not permeate and H_2 and H_2O do not have the decay loss term. V [m^3] is the volume of the control volume, c [$mol\,m^{-3}$] is the species concentration, F_{in} [$mol\,s^{-1}$] is the molar flow rate entering the volume, q [$m^3\,s^{-1}$] is the volumetric flow rate, J_p [$mol\,m^{-2}\,s^{-1}$] is the permeation flux through the surface of area A [m^2], λ [s^{-1}] is the decay constant, ω [s^{-1}] is the leak rate and δ_{Ch} [$mol\,s^{-1}$] is reaction rate related to Eq. (2).

$$V\frac{\partial c_{HT}}{\partial t} = F_{in,HT} - qc_{HT} - J_{p,HT}A - \lambda V c_{HT} - \omega V c_{HT} - \delta_{Ch} \tag{3}$$

At the fluid-wall interface, under the assumption of equilibrium conditions, Eqs. (4) and (5) are used for the heteronuclear molecule HT and the homonuclear molecule H_2, to equate hydrogen partial pressures on the two sides [12]. Here, the subscripts f and s denote the same interface on the fluid and on the solid side, respectively. $K_{s,f}$ [$mol\,m^{-3}\,Pa^{-1}$] is the solubility in water and K_s [$mol\,m^{-3}\,Pa^{0.5}$] is the one in structures. Diffusion in walls is done using an implicit, second order accurate and unconditional stable numerical method (Crank–Nicolson).

$$\frac{c_{HT,f}}{K_{s,f}} = 2\frac{c_{H,s}c_{T,s}}{K_s^2} \tag{4}$$

$$\frac{c_{H_2,f}}{K_{s,f}} = \left(\frac{c_{H,s}}{K_s}\right)^2 \tag{5}$$

In [13] authors conducted a comprehensive system-wide analysis of tritium transport and addressed integration challenges related to the breeding blanket and other ancillary components. Based on the outcomes of this study, a uniform and constant tritium source reproducing losses from the lead–lithium towards the PHTS is considered. Due to the absence of leak data for the EU DEMO BB PHTS, input data have been assumed from a literature review. A value of $1.42\,kg\,h^{-1}$ [14] has been assumed for leaks from the PHTS to the PCS. For leak rates from the PHTS to the tokamak building rooms, values from literature for fission machines range between $0.1\,kg\,h^{-1}$ and $1.9\,kg\,h^{-1}$ [15–17]. A conservative value of $2.0\,kg\,h^{-1}$ has been chosen. These leaks are modelled as constant loss terms from the hydrodynamic volumes and are divided over all the pipe volumes based on the ratio between the water inventory in each volume and the loop's total inventory.

H_2 concentration is fixed by the coolant chemistry control strategy to minimize oxidation. From the point of view of permeation from the BB to the primary coolant, it might seem beneficial to increase H_2 content in the coolant. This would lead to an increase in tritium partial pressure on the coolant side, resulting in a reduction of concentration gradient between the BB and the PHTS. On the other hand, for the same reason, this would increase the concentration gradient between the PHTS and the rooms, leading to a potential increase in losses towards the rooms.

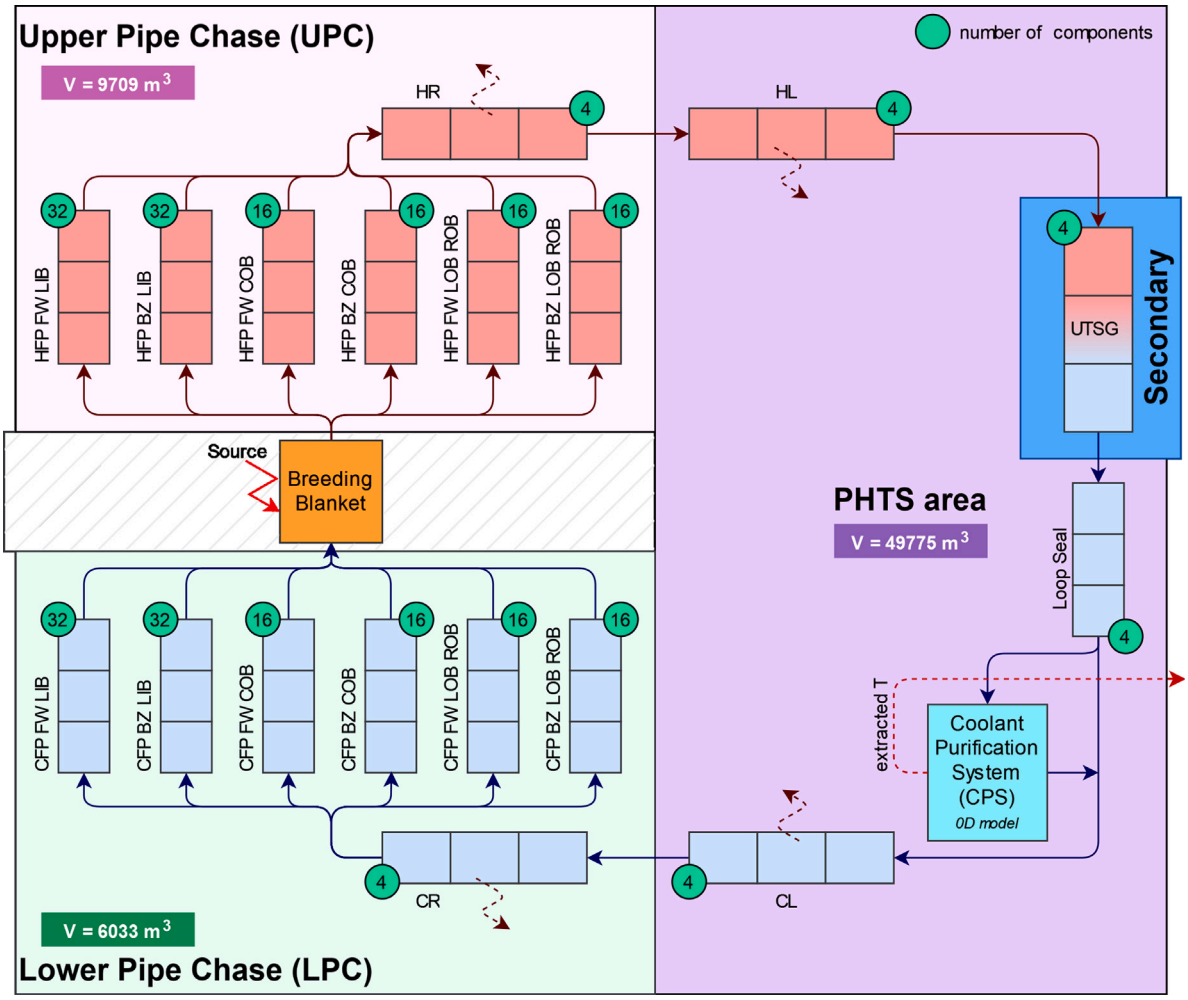

Fig. 1. DEMO WCLL BB PHTS piping and Tokamak Rooms SAETTA nodalization.

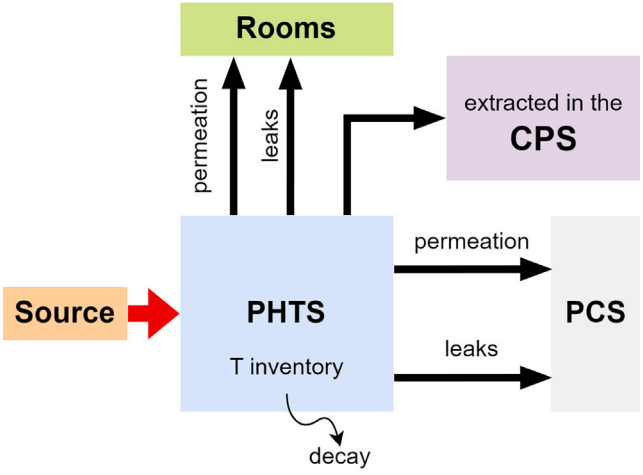

Fig. 2. Tritium pathways in the BB PHTS.

For water, the reaction rate related to Eq. (2) is obtained using the equilibrium constant (K_{eq}) from [18] and Eq. (6), where $\dot{M}$ [mol s^{-1}] is the molar mass flow rate. Hydrogen diffusivity and solubility in water are taken from [19] and [20], respectively.

$$\frac{\left(\dot{M}_{H_2}+\delta_{Ch}\right)\left(\dot{M}_{HTO}+\delta_{Ch}\right)}{\left(\dot{M}_{HT}-\delta_{Ch}\right)\left(\dot{M}_{H_2O}-\delta_{Ch}\right)}=K_{eq} \tag{6}$$

Hydrogen transport properties for stainless steel 316L from [21] are used for the piping. The diffusivity of tritium in Inconel 600, considered for steam generator tubes, is taken from [22], while solubility and hydrogen diffusivity are taken from [23].

All three rooms considered are at a temperature of 30 °C and pressure of 98 kPa [24]. Rooms volumes are shown in the model nodalization (Fig. 1).

3. Input data

3.1. EU DEMO WCLL BB PHTS design reference

This work focuses on the WCLL BB concept, where Li^6 enriched Lead–Lithium alloy acts as neutron multiplier and tritium breeder, while cooling is done by pressurized water in the PHTS. The reference system design is the 2017 DEMO Baseline with 2 GW of fusion power [25] and the latest system architecture and layout has been considered. The system operates with pressurized water at 15.5 MPa, cools both the First Wall (FW) and the Breeding Zone (BZ), and is comprised of two connected loops, each one enveloping the whole tokamak feeding the even and odd segments in an alternating way (eight BB segments per loop). The loops are in turn divided in two subsections, each one associated with half tokamak, i.e., providing the

Table 1
Piping housed in each of the tokamak building rooms related to the BB PHTS.

Room	Piping
PHTS area	HL, CL SGs
LPC	CFP FW LIB, CFP BZ LIB CFP FW COB, CFP BZ COB CFP FW LOB ROB, CFP BZ LOB ROB
UPC	HFP FW LIB, HFP BZ LIB HFP FW COB, HFP BZ COB HFP FW LOB ROB, HFP BZ LOB ROB

Table 2
Simulation parameters.

Parameter	Ref. value	Sensitivity
BB source [$mg_T\ d^{-1}$]	428.9	–
H_2O inventory [kg]	366 687	–
CPS flow rate [$kg\,h^{-1}$]	110	200.25
CPS efficiency [%]	83.2	89.4
Leak rate piping [$kg\,h^{-1}$]	2.0	0
Leak rate SG [$kg\,h^{-1}$]	1.41	0
PRF SG [–]	1000	1, 100
H_2 concentration [ppm]	2	20, 200, 2000, 20000
Rooms relative humidity [%]	0	10 – 90

cooling function to four segments. Considering one half of a loop, there are 32 Hot Feeding Pipes (HFPs) exiting the BB region with water at 328 °C. From there, water is collected in a Hot Ring (HR) that leads to a Steam Generator (SG) via a Hot Leg (HL). The loop seal connects the SG to one main cooling pump. The cold water then goes into one Cold Leg (CL) and then in a Cold Ring (CR), from where it is distributed in 32 Cold Feeding Pipes (CFP) to enter the BB at the temperature of 295 °C (Fig. 1).

Both HFPs and CFPs are divided into 6 types, depending on which BB segments they are connected to and if they serve the FW or the BZ. For both FW and BZ there are Left InBoard (LIB), Central OutBoard (COB) and Left OutBoard/Right OutBoard (LOB/ROB) cold and hot feeding pipes. The cooling circuits of the lateral OB segments are fed in parallel by feeding manifolds which split inside the upper port.

PHTS components are housed into the tokamak building, in three main areas (rooms). The PHTS area contains HL, CL, SGs and pumps, while the Upper Pipe Chase (UPC) and Lower Pipe Chase (LPC) contain hot and cold feeding pipes and rings, respectively (see Table 1 for a visual representation of where each piping section is located). All these rooms are kept at a pressure lower than the atmospheric one to limit losses of radioactive airborne material. Tokamak building input data are taken from [26].

3.2. Simulation parameters

A sensitivity analysis on the most relevant design parameters has been done, and these values, along with the ones used for the reference case, are reported in Table 2. Various scenarios were explored, including alternative CPS design point (CPS flow rate and efficiency), the absence of leakages, the use of less effective permeation barriers, varying hydrogen content in the water, and different hygrometric conditions within the tokamak building rooms.

The reference CPS parameters are based on a preliminary sizing that should guarantee a tritium concentration in water below $2\,Ci\,kg^{-1}$ [27]. The efficiency is defined according to Eq. (7), where in and out refer to the CPS connections to the PHTS, thus the numerator is the extraction rate.

$$\eta_{CPS} = 100 \times \frac{c_{HTO,in} - c_{HTO,out}}{c_{HTO,in}} \tag{7}$$

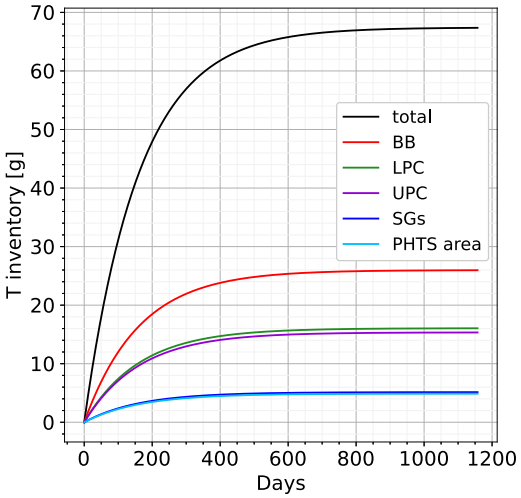

Fig. 3. Reference case: tritium inventories in the BB PHTS coolant. The inventory is broken down based on the environment faced by the different piping sections.

4. Results and discussion

In this section, simulation results are shown and commented. The reference case is first presented, followed by a subsection dedicated to each sensitivity.

4.1. Reference case

The case is initialized at steady state thermal-hydraulic conditions (temperatures, densities, flow rates) and with a fixed and uniform H_2 concentration. HT and HTO concentrations in fluids and H and T concentrations in metals are initialized to zero. Also the tritium partial pressure in the rooms is set to zero. Pipes and UTSGs tubes temperatures are conservatively set equal to the one in the primary water coolant throughout their thickness. For UTSGs a linear temperature gradient in the bulk of the fluid is assumed. The simulation runs for the duration of the entire plasma operating sequence (~ 2.8 years) [28] and the CPS extraction rate with respect to what it receives from the PHTS (i.e., the efficiency defined in Eq. (7)) is considered at its nominal value from the beginning of the simulation.

An overview of tritium inventories and permeation/leakage rates is given in Section 4.1.1, while in Section 4.1.2 the evolution of tritium concentration and activity (both gaseous and liquid) in the PHTS rooms is analysed.

4.1.1. Tritium rates and inventories

Steady state is almost reached after ~ 2.8 years of continuous operation with constant source term and sinks. Fig. 3 shows the total coolant tritium inventory (black line) and the inventory in the piping inside the BB (red line), facing the PHTS rooms (green for the LPC, purple for the UPC and cyan for the PHTS area) and in the SGs tubes (i.e., facing the PCS, blue line). The overall tritium inventory within the PHTS reaches about 67.4 grams, of which the biggest contributor is the portion in the BB followed by lower and upper pipe chase. The contribution of each piping segment to the overall inventory is directly proportional to the water inventory in the piping itself. In fact, tritium concentration is uniform throughout the PHTS at $1.78\,Ci\,kg^{-1}$, respecting the limit of $2\,Ci\,kg^{-1}$ imposed in the CPS design.

Coolant inventory in the piping facing the LPC is slightly higher than the one in the piping facing the UPC due to lower volumetric flow rates in the cold side of the loop. The rate at which inventory builds up and the final inventory are strictly related to the bypass flow rate sent to the CPS and its efficiency curve, as it will be shown in Section 4.3. This can

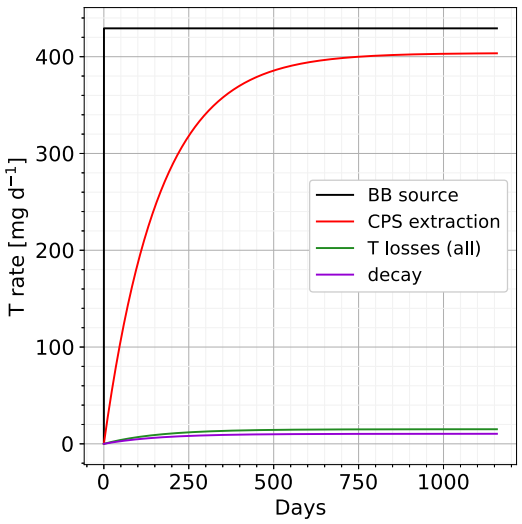

Fig. 4. Reference case: tritium balance in the BB PHTS over time.

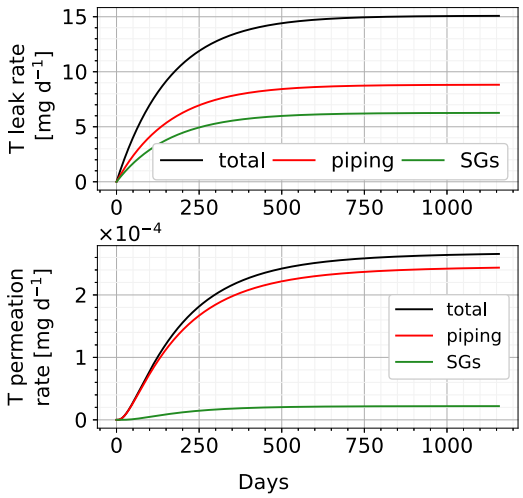

Fig. 5. Reference case: tritium losses from the piping and from the SGs due to leakage (upper plot) and permeation (lower plot).

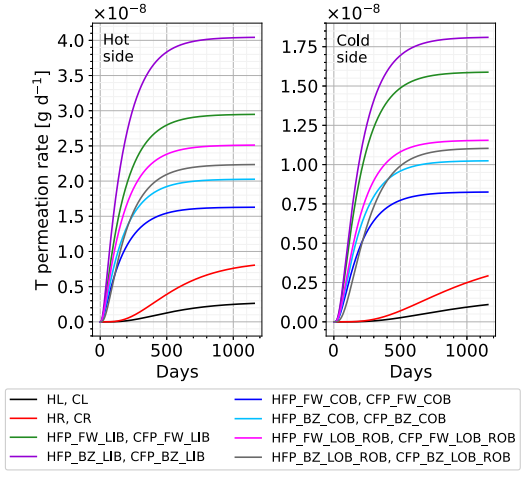

Fig. 6. Reference case: tritium permeation rates from all pipes. On the left are shown components at 328 °C and on the right components at 295 °C.

also be seen in Fig. 4, where the main tritium rates contributing to the tritium balance within the PHTS are shown. With respect to the PHTS, the BB source (indicated by the black line) is the only positive term, while the other quantities represent sinks. They are shown as positive for improved graphical clarity.

The shape of the red line, representing the rate of tritium extracted in the CPS, is the same as that of the total inventory in Fig. 3, and shows how the coolant purification is by far the most relevant tritium pathway for the coolant inventory. The source term coming from the lead–lithium loop in the BB is constant, while T losses, computed as the sum of all leaked and permeated T, are shown in green. Decaying T is shown in purple. At the end of the simulation, the T extracted from the CPS accounts for about 96% of the source rate, while the remaining 6% goes into leakages, permeation and decay.

A focus on the losses shown in Fig. 4 is made in Fig. 5, distinguishing between HT and HTO leaks (top plot) and HT permeation (bottom plot). Leaks are by far the dominant loss rate, surpassing permeation rates by five orders of magnitude. While SGs contribution (green line) to leakage are comparable to the piping one (red line) due to the assumed leak rates, the reference PRF maintains permeation losses towards the balance of plant at a significantly lower level than the overall permeation loss from the rest of the piping.

For each section of the piping, depending on the piping surface to water volume ratio, a different permeation transient is observed. In Fig. 6 tritium permeation rates over time from the hot pipes (left plot) and cold pipes (right plot) are shown.

It can be seen how the HR (red line, left plot), HL (black line, left plot), CR (red line, right plot) and CL (black line, right plot), the four piping sections with the smaller surface to volume ratio, are still experiencing a growth in permeation rate while CFPs and HFPs (characterized by higher ratios) have achieved steady state conditions. Furthermore, it is possible to observe a higher permeation rate from the piping on the hot side of the loop (solid lines) compared to the cold side (dashed lines) due to the lower permeability of the steel at lower temperatures.

4.1.2. Tritium concentration and activity in PHTS rooms

Mitigation strategies in the rooms are yet unknown. The assumption of fixed relative humidity in the rooms made in this work can be seen as having dryers that work both as dryers (i.e., they remove water vapour from the room) and as tritium removal systems (leaked HTO is removed along with H_2O). For each room, the inventory build-up will mainly depend on the loss rate from the piping housed in the room (see Table 1), which in turn depends on the leak rate, on the permeation flux and on the surface of piping exposed to the room's atmosphere. This is evident in Fig. 7, where the UPC (black dash-dotted line in Fig. 7) and LPC (red dash-dotted line in Fig. 7) show the largest growth in air concentration over time due to much larger permeation rates from the piping they house (see Fig. 6). The same trend can be seen in Fig. 8, showing the activity in the rooms due to HT permeation and leakage (top plot) and due to HTO leakage (bottom plot). The activity in the rooms can be attributed nearly entirely to the leaked HTO.

The build-up of activity within the rooms' atmospheres due to the loss of HT is presented in the top plot of Fig. 8, while the bottom plot illustrates the activity in the liquid phase resulting from the loss of HTO. The activity due to HTO is orders of magnitude larger than that of HT, and this should be taken into account during the design of room mitigation strategies and tritium management systems. The objective of this analysis is not to model detailed dynamics between the gaseous and liquid phases and the hydrogen isotopologues, but rather to estimate the potential amount of tritium that may accumulate in the tokamak building rooms associated with the PHTS. In this sense, the activity due to HTO can be a load to both the EDS and Water Detritiation System (WDS), with a different contribution to the former rather than to the latter depending on the mitigation strategies devised for the rooms.

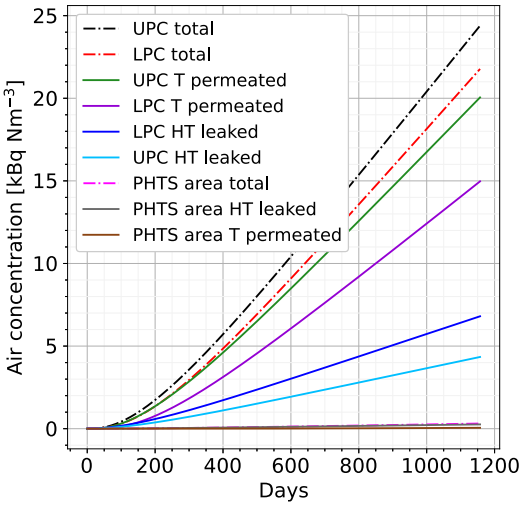

Fig. 7. Reference case: air concentration in tokamak building rooms due to leakage and permeation from the BB PHTS.

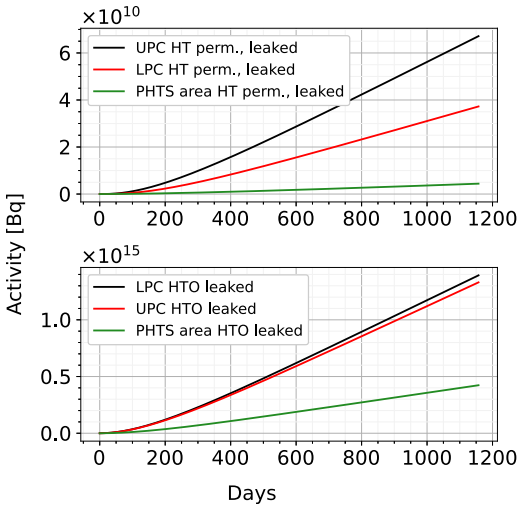

Fig. 8. Reference case: activity in gaseous (air, top plot) and liquid (bottom plot) phase in PHTS rooms.

Ultimately, this activity will be found in the sump tanks of the rooms and/or in the dryers.

From the point of view of the activity in the atmosphere, it is of interest to verify whether or not a certain concentration threshold for EDS activation is reached. Such a threshold will be ultimately defined via dedicated studies combining EDS and safety features. Preliminary activities performed in KDII #2 and #6 have identified the tritium concentration threshold of 10^8 Bq Nm^{-3} inside a room to switch the ventilation from HVAC to EDS. We already know that for the reference relative humidity (Φ) of 0% the concentration in the rooms is far from the threshold, but from this point of view a higher Φ would lead to higher tritium content in the gaseous phase due to the presence of vapour HTO. A sensitivity on the Φ in the PHTS area has been done assuming that the ratio of HTO to H_2O in the vapour phase is the same of that in the liquid phase and results are shown in Fig. 9. Even in the case of Φ = 90% (light green curve) the EDS activation threshold is not reached.

Another value of interest concerning tritium concentration in the rooms is the Derived Air Concentration (DAC), defined as the airborne concentration that equals the annual limit of intake divided by the volume of air breathed by an average worker for a working year [29].

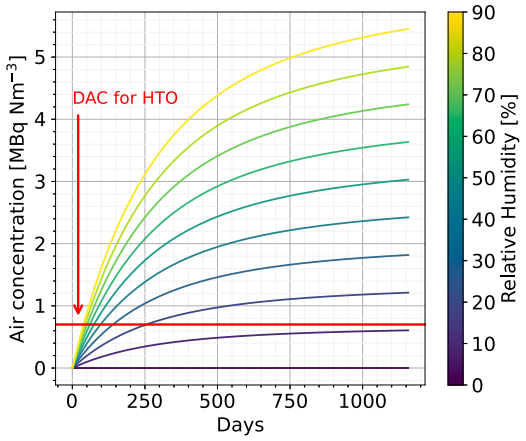

Fig. 9. Air concentration in the PHTS area due to tritium losses from the BB PHTS at different relative humidities. The horizontal red line shows the DAC for tritiated water.

Table 3
Time it takes in days to exceed the DAC for tritiated vapour in the tokamak building rooms housing the BB PHTS.

Φ[%]	Days to exceed 7×10^5 Bq Nm^{-3}
0	–
10	–
20	255
30	140
40	97
50	74
60	60
70	51
80	44
90	39

The DAC for tritiated water is 7×10^5 Bq Nm^{-3}, while for the non oxidated form is 9×10^9 Bq Nm^{-3} [29]. Considering HTO, the limit is not exceeded only up to Φ = 10%. Above 10% Φ, increasing the Φ shortens the time required to exceed the value, as shown in Table 3.

4.2. No-leakage case

If there are no leaks throughout the water loop, only permeation contributes to losses. Tritium concentration in the loop increases by 3.6% at the end of the simulation, leading to an analogous increase in overall inventory and tritium mass flow rate going to the CPS. Although permeation increases, the absence of leaked HT causes a significant decrease in the tritium contents of the rooms atmospheres, while the liquid HTO inventory is zero.

4.3. Alternative CPS configuration

The use of a larger and more efficient CPS, capable to elaborate 200.25 kg h^{-1} of coolant [27] with an efficiency of 89.4%, has a strong effect on tritium accumulation and migration in the PHTS and related rooms. As it can be seen in Fig. 10, using this CPS configuration the steady state inventory is achieved sooner, and the tritium mass flow rate going to the CPS increases with respect to the reference case due to a decrease in losses. The decrease in losses is caused by the reduced tritium concentration in water, which goes down by about 47% to a value of 0.94 Ci kg^{-1} at the end of the simulation. This value is coherent with the CPS design here under analysis, sized to maintain the concentration within 1.0 Ci kg^{-1}.

4.4. The effect of H_2 concentration

In addition to the reference value of 2 ppm, several values of H_2 concentration have been investigated, ranging from 20 to 20000 ppm.

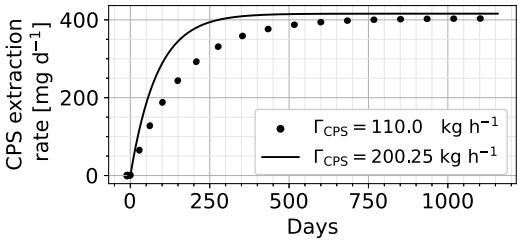

Fig. 10. Comparison of the CPS extraction rate between the reference case (REF, dotted line) and the case with a CPS sized to maintain tritium concentration in PHTS water below 1.0 Ci kg^{-1} (CPS sens, solid line).

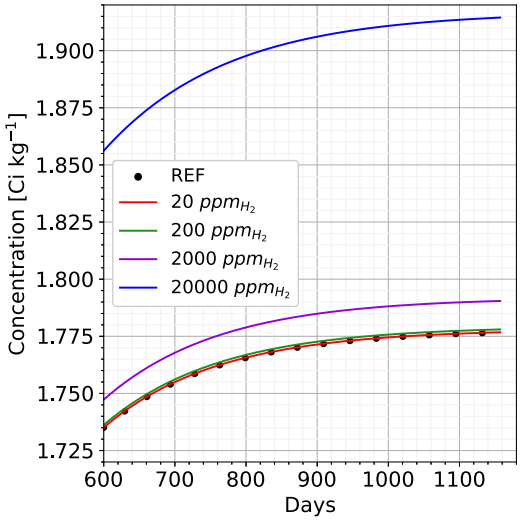

Fig. 11. Tritium concentration in the PHTS coolant at different H_2 concentrations. The reference line (black dots) is obtained with 2 ppm of H_2.

From the perspective of tritium behaviour, an increase in H_2 concentration leads to a partial transition from HTO to HT (Eq. (2)). It is important to note that the majority of tritium is initially in HTO form. Consequently, the difference is marginally perceptible for HTO but becomes substantially significant for HT, particularly when the H_2 concentration exceeds 2000 ppm.

Fig. 11 shows the overall effect on tritium concentration in the water for increasing concentrations of H_2, which becomes significant starting from 2000 ppm of H_2. The decrease in HTO concentration leads to a decrease in the extraction rate by the CPS (responsible for purifying water from HTO but not from HT).

The shift in species causes also an overall increase in tritium losses, with a marginally smaller HTO leak rate and an ever increasing HT concentration. Consequently, HT leak and permeation rate (bottom plot in Fig. 12) increase with increasing concentrations of H_2. From the top plot in Fig. 12 it can be seen how the net effect on leakage contribution is a small increase, noticeable only from 20000 ppm of H_2. Nonetheless, it can be seen from Fig. 12 that HTO leaks (top plot) still dominate over permeation (bottom plot). The combined effect of all these mechanisms results in a small increase in tritium concentration in the water, as shown in Fig. 11. The larger HT losses cause an increase of the air activity in the rooms (humidity is removed by the dryers). The increase in air concentration in the rooms for increasing H_2 concentration in the water is significant and the net observed effect is that less tritium is removed by the dryers and more is found as HT. In the worst case analysed, namely the one with 20000 ppm of H_2, the concentration in the air of the UPC (the room that displays the highest concentration) exceeds 4.0×10^7 Bq Nm^{-3} at the end of the simulation. This value is about five orders of magnitude more than the reference case but is still

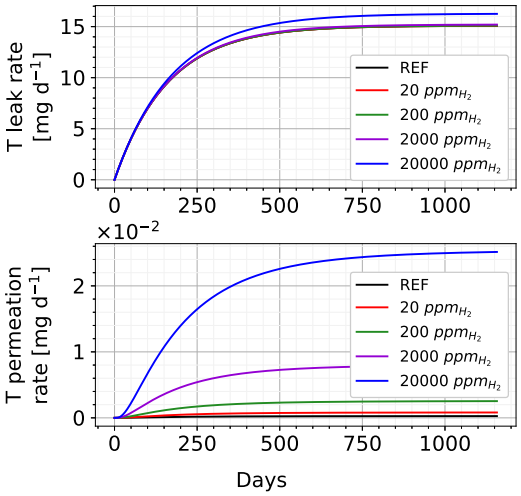

Fig. 12. Tritium leak rate (top plot) and permeation rate (bottom plot) at different H_2 concentrations.

under the EDS activation threshold. Furthermore, at the reference Φ, this concentration in the air is caused by tritium in gaseous form, thus neither the DAC for tritium in elemental form nor that for the oxidized form are surpassed.

4.5. The effect of the SG PRF

The only notable effect caused by the decrease of the SG PRF is an increase in permeation rate towards the balance of plant. The total permeation rate at the SG in the case of PRF 1 and 100 are of the order of 2.2×10^{-2} and 4.5×10^{-4} mg d^{-1}, respectively. These values are still significantly smaller than the leakage losses, of the order of 15 mg d^{-1}.

5. Conclusions

A comprehensive system-level analysis of tritium transport within the EU DEMO WCLL BB PHTS and its associated rooms has been conducted using the SAETTA code. The developed model enables the estimation of tritium (HT, HTO) concentration in the coolant under transient conditions, assessed on a component-by-component basis. Furthermore, the model allows the estimation of tritium loss rates into the surrounding rooms housing the BB PHTS, specifically the Upper Pipe Chase, Lower Pipe Chase, and PHTS area. The analysis also includes an examination of the effects of relative humidity in these rooms, as well as the implications of various factors, including the size of the Coolant Purification System, the Permeation Reduction Factor of the Heat Exchangers tubes, leakage rates, and the concentration of molecular hydrogen (H_2) in the coolant.

After almost 3 years of continuous operation with constant source term, a proper steady state is not yet reached and tritium inventory in the coolant is about 67.4 grams, equally distributed in the various sections of the loop depending on the water inventory. In fact, tritium concentration in the water is practically constant throughout the system and the presence of the CPS does not alter it significantly, due to the small fraction of flow rate elaborated. Sections with a small surface to volume ratio (i.e., large tubes) are still experiencing a transient in permeation flux that will be smaller, at steady state, of smaller pipes with a higher ratio. Furthermore, permeation from the hot section of the loop is higher than the cold part. For these reasons, the build-up of tritium in the air of the UPC is similar but higher than that in the LPC, and they are both significantly larger than that in the PHTS area (which, permeation-wise, houses only the hot and cold legs). Nonetheless, tritium in the coolant primarily exists in the form of HTO.

The impact of leakages is significantly greater than that of permeation losses, with leakages being several orders of magnitude larger.

The size of the CPS is the main factor influencing the evolution of tritium concentration within the loop. Implementing a larger and more efficient CPS results in a reduction of tritium inventory in the coolant, which corresponds to decreased loss rates and an increased extraction rate by the CPS. The concentration of tritium in the air within the rooms, resulting from leakage and permeation losses from the PHTS system, is significantly influenced by the target relative humidity maintained by the dryers. The EDS activation threshold is never reached, even under the most unfavourable conditions of elevated relative humidity. On the other hand, the DAC for tritiated vapour is surpassed after 255 days if the relative humidity is maintained at 20%, and in less days if the target relative humidity is higher. Increasing the H_2 concentration in the water causes a transfer of tritium from HTO to HT. This in turn leads to a reduction in the extraction rate by the CPS and an increase in tritium concentration in the coolant, along with losses from the piping. Although HT losses become considerably more pronounced, it is important to note that in the worst case scenario analysed where the coolant contains 20000 ppm of H_2, the activity levels within the rooms remain below the EDS activation threshold and below the DAC.

Following the present analysis, the tritium loads from the PHTS to the CPS and PHTS-related rooms have been estimated. These values will be instrumental in the definition of tritium management and room ventilation strategies, and will help in the design of large and costly fuel cycle components such as the Exhaust Detritiation System and the Water Detritiation System.

Symbols

A	(m^2) area
C	($mol\,m^{-3}$) concentration
δ_{ch}	($mol\,s^{-1}$) molar variation
F_{in}	($mol\,s^{-1}$) inlet flow rate
J_p	($mol\,m^{-2}\,s^{-1}$) permeation flux
K_{eq}	(−) equilibrium constant
K_s	($mol\,m^{-3}\,Pa^{-0.5}$) solubility in metals
$K_{s,f}$	($mol\,m^{-3}\,Pa^{-1}$) solubility in fluids
$\dot{M}$	($mol\,s^{-1}$) molar flow rate
q	($m^3\,s^{-1}$) volumetric flow rate
V	(m^3) volume
λ	(s^{-1}) tritium decay constant
ω	(s^{-1}) leak rate

Acronyms

BB Breeding Blanket

BoP Balance of Plant

BZ Breeding Zone

CFP Cold Feeding Pipe

CL Cold Leg

COB Central OutBoard

CPS Coolant Purification System

CR Cold Ring

DAC Derived Air Concentration

EDS Exhaust Detritiation System

EU DEMO European DEMOnstration power plant

FW First Wall

HCPB Helium-Cooled Pebble Bed

HFP Hot Feeding Pipe

HL Hot Leg

HR Hot Ring

KDII key Design Integration Issues

LIB Left InBoard

LOB Left OutBoard

LPC Lower Pipe Chase

PCS power Conversion System

PHTS Primary Heat Transfer System

PRF Permeation Reduction Factor

ROB Right OutBoard

SAETTA System-lvl App. for Engineering Tritium Transport Analysis

SG Steam Generator

UPC Upper Pipe Chase

UTSG U-Tube Steam Generator

WCLL Water-Cooled Lead-Lithium

WDS Water Detritiation System

CRediT authorship contribution statement

Federico Hattab: Writing – review & editing, Writing – original draft, Visualization, Software, Methodology, Investigation, Formal analysis, Data curation, Conceptualization. **Vincenzo Narcisi:** Writing – review & editing, Supervision, Methodology, Formal analysis. **Cristiano Ciurluini:** Writing – review & editing, Supervision, Resources. **Fabio Giannetti:** Writing – review & editing, Supervision, Funding acquisition. **Giulia Valeria Centomani:** Funding acquisition. **Antonio Trotta:** Funding acquisition. **Alessia Santucci:** Writing – review & editing, Supervision, Project administration, Methodology.

Declaration of competing interest

The authors declare that they have no known competing financial interests or personal relationships that could have appeared to influence the work reported in this paper.

Acknowledgments

Project ECS 0000024 Rome Technopole, - CUP B83C22002820006, NRP Mission 4 Component 2 Investment 1.5, Funded by the European Union - NextGenerationEU.

This work has been carried out within the framework of the EUROfusion Consortium, funded by the European Union via the Euratom Research and Training Programme (Grant Agreement No 101052200 — EUROfusion). Views and opinions expressed are however those of the author(s) only and do not necessarily reflect those of the European Union or the European Commission. Neither the European Union nor the European Commission can be held responsible for them.

Data availability

Data will be made available on request.

References

[1] John Wesson, David J. Campbell, Tokamaks, Oxford University Press, 2011.

[2] Alessia Santucci, Marco Incelli, Leonardo Noschese, Carlos Moreno, F. Di Fonzo, Marco Utili, Silvano Tosti, Christian Day, The issue of tritium in DEMO coolant and mitigation strategies, Fusion Eng. Des. 158 (2020) 111759.

[3] C. Bachmann, S. Ciattaglia, F. Cismondi, G. Federici, T. Franke, C. Gliss, T. Härtl, G. Keech, R. Kembleton, F. Maviglia, M. Siccinio, Key design integration issues addressed in the EU DEMO pre-concept design phase, Fusion Eng. Des. 156 (2020) 111595.

[4] F. Franza, A. Ciampichetti, I. Ricapito, M. Zucchetti, A model for tritium transport in fusion reactor components: The FUS-TPC code, Fusion Eng. Des. 87 (4) (2012) 299–302.

[5] Elisabeta Carella, Carlos Moreno, Fernando Roca Urgorri, David Rapisarda, Angel Ibarra, Tritium modelling in HCPB breeder blanket at a system level, Fusion Eng. Des. 124 (2017) 687–691, Proceedings of the 29th Symposium on Fusion Technology (SOFT-29) Prague, Czech Republic, September 5-9, 2016.

[6] Leonardo Noschese, Alessia Santucci, Silvano Tosti, Francesco Romanelli, Tritium permeation modelling in DEMO WCLL cooling system, Fusion Eng. Des. 161 (2020) 112046.

[7] Luigi Candido, Marco Utili, Iuri Nicolotti, Massimo Zucchetti, Tritium transport in HCLL and WCLL DEMO blankets, Fusion Eng. Des. 109–111 (2016) 248–254, Proceedings of the 12th International Symposium on Fusion Nuclear Technology-12 (ISFNT-12).

[8] I. Fernández-Berceruelo, I. Palermo, F.R. Urgorri, D. Rapisarda, M. González, J. Alguacil, J.P. Catalán, J.M. García, J. Kekrt, M. Kordač, I. Krastiņš, T. Melichar, J.Á. Noguerón, E. Platacis, R. Petráš, M. Roldán, A. Rueda, J. Serna, D. Sosa, D. Suàrez, Progress in design and experimental activities for the development of an advanced breeding blanket, Nucl. Fusion 64 (5) (2024) 056029.

[9] F. Hattab, V. Narcisi, C. Ciurluini, A. Trotta, A. Santucci, F. Giannetti, Multifunctional code for hydrogen isotopes transport analyses: verification and validation against fusion-relevant applications, Nucl. Fusion 65 (2) (2025) 026062.

[10] Yannick Nicolas Hörstensmeyer, Holistic fuel cycle modelling of a future fusion reactor=Holistische Modellierung des Brennstoffkreislaufs eines zukünftigen Fusionsreaktors (Ph.D. thesis), Karlsruher Institut für Technologie (KIT), 2022, 31.99.01; LK 01.

[11] Jonas Caspar Schwenzer, A Process Simulator for the Prediction and Optimization of the Operation of the Fuel Cycle of a Fusion Power Plant (Ph.D. thesis), Karlsruher Institut für Technologie (KIT), 2024.

[12] Glen Rs Longhurst, TMAP7 User Manual, Technical Report, Idaho National Engineering and Environemntal Laboratory, Idaho Falls, ID (United States), 2008.

[13] G.A. Spagnuolo, R. Arredondo, L.V. Boccaccini, P. Chiovaro, S. Ciattaglia, F. Cismondi, M. Coleman, I. Cristescu, S. D'Amico, C. Day, A. Del Nevo, P.A. Di Maio, M. D'Onorio, G. Federici, F. Franza, A. Froio, C. Gliss, F.A. Hernández, A. Li Puma, C. Moreno, I. Moscato, P. Pereslavtsev, M.T. Porfiri, D. Rapisarda, M. Rieth, A. Santucci, J.C. Schwenzer, R. Stieglitz, S. Tosti, F.R. Urgorri, M. Utili, E. Vallone, Integrated design of breeding blanket and ancillary systems related to the use of helium or water as a coolant and impact on the overall plant design, Fusion Eng. Des. 173 (2021) 112933.

[14] T. Chandrasekaran, J.Y. Lee, C.A. Willis, Calculation of releases of radioactive materials in gaseous and liquid effluents from pressurized water reactors (PWR-GALE code). Revision 1, 1985.

[15] AP1000 European Design Control Document. In Chapter 12-Radiation Protection, Technical Report, Westinghouse Electric Company LLC, 2009.

[16] Mitsubishi Heavy Industries Ltd., Design Control Document for the US-APWR, Chapter 12, MUAP-DC012, Rev. 4, Technical Report, 2013.

[17] K.Y. Wong, T.A. Khan, F. Guglielmi, Canadian Tritium Experience, Canadian Fusion Fuels Technology Project, 1984.

[18] Michiko Ahn Furudate, Seungyon Cho, Denis Hagebaum-Reignier, Study on chemical kinetics of HTO + H2 -> H2O + HT for design of tritium breeding blanket, Fusion Eng. Des. 136 (2018) 438–441, Special Issue: Proceedings of the 13th International Symposium on Fusion Nuclear Technology (ISFNT-13).

[19] Dimitrios T. Kallikragas, Andriy Y. Plugatyr, Igor M. Svishchev, High temperature diffusion coefficients for O2, H2, and OH in water, and for pure water, J. Chem. Eng. Data 59 (6) (2014) 1964–1969.

[20] Jorge Alvarez, Rosa Crovetto, Roberto Fernández-Prini, The dissolution of N2 and of H2 in water from room temperature to 640 K, Berichte der Bunsenges. Für Phys. Chem. 92 (8) (1988) 935–940.

[21] K.S. Forcey, D.K. Ross, J.C.B. Simpson, D.S. Evans, Hydrogen transport and solubility in 316L and 1.4914 steels for fusion reactor applications, J. Nucl. Mater. 160 (2) (1988) 117–124.

[22] Kan Sakamoto, Masayasu Sugisaki, Diffusion coefficient of tritium in Ni-based alloy, Fusion Sci. Technol. 41 (3P2) (2002) 912–914.

[23] N. Kishimoto, T. Tanabe, T. Suzuki, H. Yoshida, Hydrogen diffusion and solution at high temperatures in 316L stainless steel and nickel-base heat-resistant alloys, J. Nucl. Mater. 127 (1) (1985) 1–9.

[24] Maria Teresa Porfiri, Alfredo Bertocchi, DEMO Room Book, Technical Report, Eurofusion Report 2NQF7B v1.0, 2019.

[25] G. Federici, C. Bachmann, L. Barucca, W. Biel, L. Boccaccini, R. Brown, C. Bustreo, S. Ciattaglia, F. Cismondi, M. Coleman, V. Corato, C. Day, E. Diegele, U. Fischer, T. Franke, C. Gliss, A. Ibarra, R. Kembleton, A. Loving, F. Maviglia, B. Meszaros, G. Pintsuk, N. Taylor, M.Q. Tran, C. Vorpahl, R. Wenninger, J.H. You, DEMO design activity in Europe: Progress and updates, Fusion Eng. Des. 136 (2018) 729–741, Special Issue: Proceedings of the 13th International Symposium on Fusion Nuclear Technology (ISFNT-13).

[26] Matteo D'Onorio, Tommaso Glingler, Maria Teresa Porfiri, Danilo Nicola Dongiovanni, Sergio Ciattaglia, Curt Gliss, Joëlle Elbez-Uzan, Pierre Cortes, Gianfranco Caruso, Development of a thermal-hydraulic model for the EU-DEMO tokamak building and LOCA simulation, Energies 16 (3) (2023).

[27] V. Narcisi, A. Santucci, Water distillation for coolant purification system of DEMO water-cooled lithium lead breeding blanket, Fusion Eng. Des. 190 (2023) 113547.

[28] Vincenzo Narcisi, Luca Tamborrini, Luca Farina, Gessica Cortese, Francesco Romanelli, Alessia Santucci, Experimental and numerical analysis of a Pd–Ag membrane unit for hydrogen isotope recovery in a solid blanket, Membranes 13 (6) (2023).

[29] 10 cfr part 835 - occupational radiation protection, Technical Report, U. S. Department of Energy, 2015.